PROCEEDINGS, 42nd Workshop on Geothermal Reservoir Engineering
Stanford University, Stanford, California, February 13-15, 2017
SGP-TR-212

An UnCoupled Radial Flow Poroelastic Model with Local Thermal (Non) Equilibrium

Mario C. Suárez-Arriaga [1] and Fernando Samaniego V. [2]

[1]Asociación Geotérmica Mexicana, 58090 Morelia, Mich. México; [2]Faculty of Engineering, UNAM, Mexico City

mcsa50@gmail.com, pexfsamaniegov01@pemex.com

Keywords: Thermo-poroelasticity, radial coupled model, local thermal non-equilibrium, cylindrical coordinates

ABSTRACT

This paper introduces a new thermo-poroelastic model in terms of analytic equations, to describe the rock deformation produced by fluid injection/extraction in geothermal reservoirs, using radial coordinates. The model is fully coupled in isothermal poroelastic conditions, but is thermally uncoupled if local thermal non-equilibrium (LTNE) is considered. The uncoupled model describes the flow of fluid and conductive-convective heat in linearly deformable porous rocks according to linear Biot's theory. The fluid flow can be of Darcy's type or non-Darcian. There are thirteen unknowns in this model: fluid pressure, variation of the fluid content in the pores, radial displacement of the solid skeleton, radial and tangential strains and stresses, porosity, deformation velocity of the solid, fluid velocity and rock and fluid temperatures, respectively. Except the temperatures, all the unknowns are explicit functions of radius and time $f(r, t)$. Considering LTNE, there is an effective volumetric heat transfer q_{sf} [W/m^3] between the solid skeleton and the liquid. The porosity is estimated as a function of fluid pressure and temperature. The radial deformation of the solid rock u_r is an irrotational vector field, as a consequence, the variation of the fluid content ζ_f, becomes proportional to the pore pressure p_f, which is calculated using the classical Theis model. In these conditions, the diffusion equation of ζ_f is integrated to obtain the solid radial displacement $u_r(r, t)$ in analytical form. The system of simultaneous equations with all its unknowns is immediately solved in cylindrical coordinates. Once the fluid velocity is obtained, the fluid temperature can be computed using a new analytical solution of the diffusion-convection equation. This radial thermoporoelastic model is didactic, useful and simple to use. It allows to explore different conditions for both the fluid and the geomechanical parameters, as well as different boundary and initial conditions; therefore, it can be used as a benchmark to test fully numerical models. Graphical results are shown to illustrate practical cases with extraction and injection of fluid into a reservoir using real data. This work is a current research in progress.

1. INTRODUCTION

Thermoporoelasticity is a branch of poromechanics that describes general thermo-hydro-mechanical phenomena (THM) (Coussy, 2004; Cheng, 2016) for real-world processes occurring when the reservoir rock is subjected simultaneously to geomechanical, thermal, hydraulic and other physical effects. The linear poroelasticity theory of M. Biot (1941-1972) is isothermal; it uses Hookean classic elasticity to describe the mechanical response of the rock, coupling Darcy's law to model the fluid transport within pores and fractures subjected to different types of stresses and boundary conditions. The processes involved in geothermal reservoirs can be isothermal or non-isothermal. In the first case, local thermal equilibrium (LTE) is assumed. The second case occur when the reservoir temperature exhibits changes, which can be assumed in LTE or under local thermal non-equilibrium conditions (LTNE). For example, this occurs when liquid is injected at lower temperature into a hot reservoir; then liquid and solid phases interact through a volumetric heat transfer mechanism (Vafai, 2015; Suárez-Arriaga, 2016). Darcy's law is influenced by rock deformation because there are changes in porosity and permeability when pressure or temperature changes. Concerning thermal diffusion, it is assumed that rock strains and darcian flow have little effect in pure heat conduction. Both situations, LTE and LTNE are formulated in this paper, but only the uncoupled radial thermoporoelastic model is solved exactly in LTE. The more general coupled LTNE model is fully outlined, however, its solution is numerical, and it will be presented in a future second part of this work. In this paper attention is focused only on rock deformation at the vicinity of a geothermal well located in a reservoir under exploitation conditions with liquid injection or fluid extraction. For this purpose, a fully coupled poroelastic analytical model in radial coordinates is developed with thermal effects uncoupled and its main outcomes are presented.

2. GEOMECHANICAL RADIAL MODEL DESCRIPTION (LTE)

Poromechanical models are necessary to compute changes of pore fluid pressure, rock strain-stress state, reinjection of cold water into hot reservoirs, deformation due to thermal changes, hydraulically or thermally induced fracturing, etc. Analytical approaches are useful to benchmark the precision and accuracy of numerical models, which are more general in scope and applicability to real world problems. Assuming the same hypothesis of the classic Theis solution to compute the transient pressure distribution in a cylindrical reservoir, it is possible to build up an exact mathematical poroelastic model, which includes fluid flow, rock deformation and temperature distribution. Supposing that all necessary coefficients can be measured, the unknowns of the radial model are thirteen. All of the unknowns, except temperatures, are functions of radius and time, having the general form [$f(r, t)$], which correspond to specific functions and equations defined in the Appendix. They are described and solved in the following algorithmic order:

1) $p_f \rightarrow$ fluid (pore) pressure. 2) $\zeta_f \rightarrow$ variation of pore fluid content. 3) $v_D \rightarrow$ Darcy velocity. 4) $u_r \rightarrow$ radial solid displacement.
5) $\varepsilon_B \rightarrow$ volumetric strain. 6) $\varepsilon_r \rightarrow$ radial strain. 7) $\varepsilon_\theta \rightarrow$ tangential strain. 8) $\varphi \rightarrow$ rock porosity. 9) $\sigma_r \rightarrow$ radial stress.
10) $\sigma_\theta \rightarrow$ tangential stress. 11) $v_S \rightarrow$ solid deformation velocity. 12) $T_f \rightarrow$ fluid temperature. 13) $T_S \rightarrow$ solid temperature.

All symbols, functions and the procedure to obtain the solutions are completely defined in the Appendix.

2.1 Governing Equations and Radial Analytic Solutions under Isothermal Conditions (LTE)

The vector displacement of the solid particles u_r (r, t) has only one spatial component acting in the radial direction and, therefore, its rotational is zero. The fluid content variation in the pores ζ_f (increment or removal) can be measured experimentally or computed from poroelastic formulae (Wang, 2000; Bundschuh & Suárez-Arriaga, 2010). Under the condition of null rotational of the vector radial displacement, the variation of the fluid content ζ_f (r, t) becomes proportional to the fluid pressure p_f (Wang, 2000; Cheng, 2016):

$$\vec{\nabla} \times \vec{u}_r(r,t) = \vec{0} \quad \Rightarrow \quad \boxed{\zeta_f(r,t) = S_r\, p_f(r,t)} \tag{1}$$

Where S_r is the uniaxial specific fluid storage in the radial direction; which is calculated in terms of the radial compressibility and other poroelastic coefficients defined in the Appendix. If the fluid pressure satisfies the geometry and hypothesis of the infinite continuous line source (see Appendix and Figure 1), then it can be computed approximately with the modified Theis solution:

$$(\text{Theis model}) \rightarrow \quad p_f(r,t) = p_0 + \frac{Q_v\,\mu_f}{4\pi z_w k_r} E_1\left[\frac{r^2}{4\eta_f t}\right] \quad \leftarrow \quad \eta_f = \frac{k_r}{\mu_f S_r} \tag{2}$$

where p_0, Q_V, μ_f, z_w, k_r, η_f are initial reservoir pore pressure, volumetric fluid flow rate, fluid viscosity, liner's length, absolute radial permeability, and hydraulic diffusivity, respectively. The symbol E_1 is the exponential integral of degree 1. From this classical solution (2) Darcy velocity v_D is deduced (gravity is neglected):

$$v_D = -\frac{k_r}{\mu_f}\frac{\partial p_f}{\partial r} = \frac{Q_v}{2\pi z_w r}\, e^{-\frac{r^2}{4\eta_f t}} \tag{3}$$

This model defined by equations (1, 2, 3) is valid for homogeneous reservoirs of radial geometry, with a fully penetrating well in a very large isotropic porous medium of thickness z_w. The main hypothesis is that the reservoir is initially a single-phase system with uniform pressure and uniform temperature everywhere.

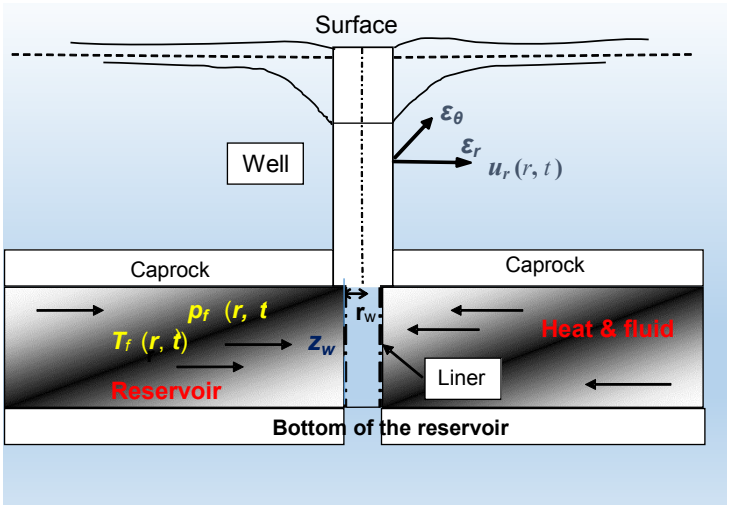

Figure 1: Reservoir geometry and main elements of the radial model. Both strains ε_r, ε_θ are related to vector u_r acting between the well's lateral boundary and the formation, along the liner's length z_w (adapted from Bundschuh & Suárez, 2010).

Once equation (1) is solved for ζ_f using the Theis solution (2), the radial displacement u_r can be integrated from the same equation (1) to obtain the following result (see Appendix), which includes the initial and radial boundary conditions at the well and at infinity:

$$\left\{\begin{matrix} u_r(r > r_w, t=0) = 0 \\ u_r(r_w, 0) = u_r(\infty, t) = 0 \end{matrix}\right\} \rightarrow \quad \boxed{u_r(r,t) = \frac{Q_v\,\gamma_e\, r}{8\pi\eta_f z_w}\left(\frac{4\eta_f t}{r^2}\left(1 - e^{\frac{-r^2}{4\eta_f t}}\right) + \Gamma_0\left[\frac{r^2}{4\eta_f t}\right]\right)} \tag{4}$$

Where γ_e is a fluid/solid coupling dimensionless parameter defined in the Appendix, Γ_0 is the incomplete Gamma function of order 0. Up to this point, four main unknown poroelastic functions, p_f, ζ_f, v_D and u_r, have been obtained as analytic functions of radius r and time t. It is assumed that the solid velocity is not negligible and can be computed using the time derivative of the displacement u_r:

$$v_s(r,t)=\frac{\partial u_r}{\partial t}=\frac{Q_v\gamma_e}{2\pi z_w r}\left(1-e^{-r^2/4\eta_f t}\right)\rightarrow\left\{v_s\left(r_w,0\right)=0;\ v_s\left(\infty,t\right)=0\right\} \tag{5}$$

The strains of the radial displacement (4) are deduced from the volumetric strain, which is the divergence of the vector displacement $\boldsymbol{u}_r$:

$$\varepsilon_r+\varepsilon_\theta=\varepsilon_B(r,t)=\nabla\cdot\left(u_r\,\underset{\Gamma}{e_r}\right)\quad\Rightarrow\left\{\varepsilon_r=\partial u_r/\partial r,\ \varepsilon_\theta=u_r/r\right\} \tag{6}$$

The effective porosity φ can be computed using the following formula (Coussy, 2004; Bundschuh & Suárez-Arriaga, 2010):

$$\varphi(r,t)=\varphi_0+b\,\varepsilon_B(r,t)+\frac{p_f(r,t)-p_0}{N_b}+\gamma_\varphi\left(T-T_0\right) \tag{7}$$

Where φ_0, N_b, γ_φ and T_0 are initial porosity, Biot tangent modulus, thermal expansion coefficient pores, and initial temperature respectively. Models for $T(r)$ and all symbols are defined in the Appendix. In radial coordinates, the stress tensor relating vertical, radial and tangential stresses and strains is (Bundschuh & Suárez-Arriaga, 2010):

$$\sigma_j=\lambda\varepsilon_B+2G\varepsilon_j-b\left(p_f-p_0\right)-K_B\gamma_B\left(T-T_0\right),\ j=r,\theta \tag{8}$$

Where λ and G are Lamé moduli, b is the Biot-Willis (1957) coefficient and γ_B is the bulk rock thermal expansivity. Once both strains are known from equation (6), the corresponding stresses are computed using equation (8), which includes the effect of both p_f and temperature changes in the fluid.

2.2 Poroelastic Results from the Isothermal Radial Model with Fluid Extraction

Assuming there are no temperature changes ($T = T_0$), the following graphics were obtained with the radial model herein described. Figures 2 illustrate the evolution of the fluid pressure radial distribution and Darcy velocity for a fluid flow rate of - 0.05 m^3/s. Total simulation time is around one hour to observe the early response. Note that the fluid discharge becomes steady state quickly, because the pressure radial gradient becomes almost constant after a short time of fluid extraction. Figures 3 show both, the distribution of $\zeta_f(r,t)$ and of $\varphi(r,t)$ produced by the flow rate, according to equations (1) and (7). The parameters used to obtain the results are in Table 1.

Table 1. Fundamental Poroelastic coefficients of the isothermal fluid/rock system

	φ_0 (ad)	k_r 10^{-13} m^2	K_B 10^9 Pa	λ 10^9 Pa	ν_U (ad)	b (ad)	G 10^9 Pa	B (ad)	K_v 10^9 Pa	γ_e (ad)	S_r 10^{-11} Pa^{-1}	γ_B 10^{-5} $°C^{-1}$
ROCK	**0.163**	**1.0**	**24.2**	**16.4**	**0.31**	**0.47**	**11.6**	**0.21**	**39.67**	**0.133**	**8.916**	**5.0**
	T_0 °C	p_0 bar	ρ_f kg/m^3	h_f kJ/kg	μ_f 10^{-6} Pa.s	K_T W/m/K	C_f 10^{-12} Pa^{-1}	c_p J/kg/K	M_b 10^9 Pa	C_b 10^9 Pa	Q_V m^3/s	γ_φ 10^{-4} $°C^{-1}$
FLUID	**50**	**50**	**990.2**	**213.6**	**544.2**	**0.643**	**438**	**4169.6**	**11.9**	**5.59**	**± 0.05**	**1.7**

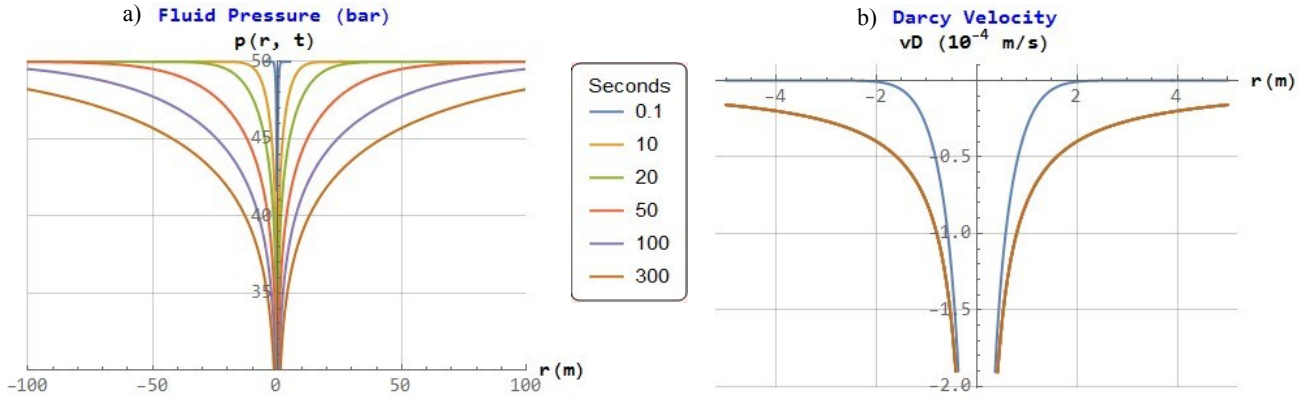

Figure 2: Fluid pressure (left) and radial Darcy velocity distribution (right) around the well, between 0.1 and 300 seconds.

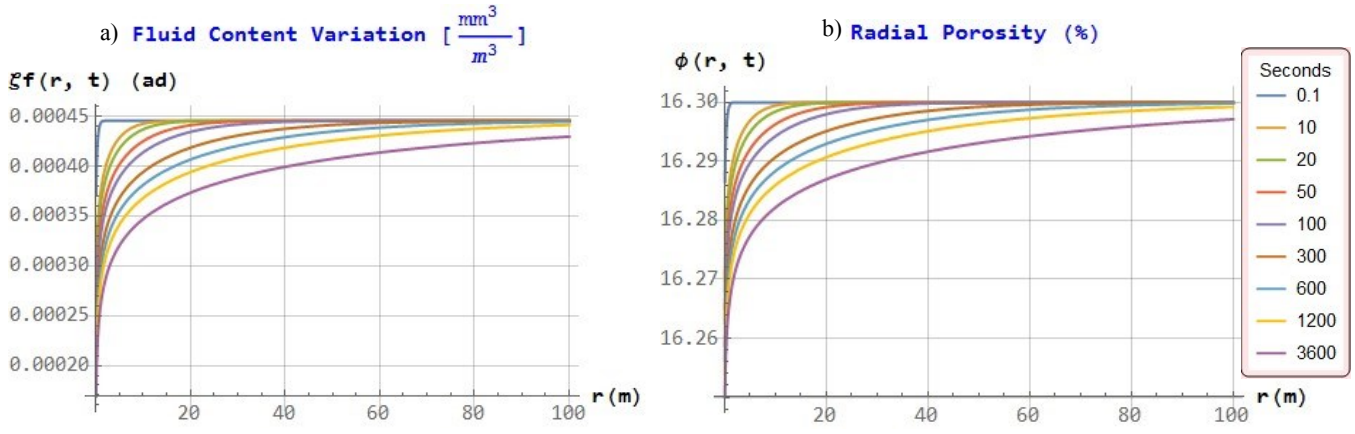

Figure 3: Fluid content removal (left) and rock porosity reduction (right). Both simulation times are between [0.1, 3600] seconds in order to observe the rapid initial poroelastic variations (reductions) produced by the fluid extraction.

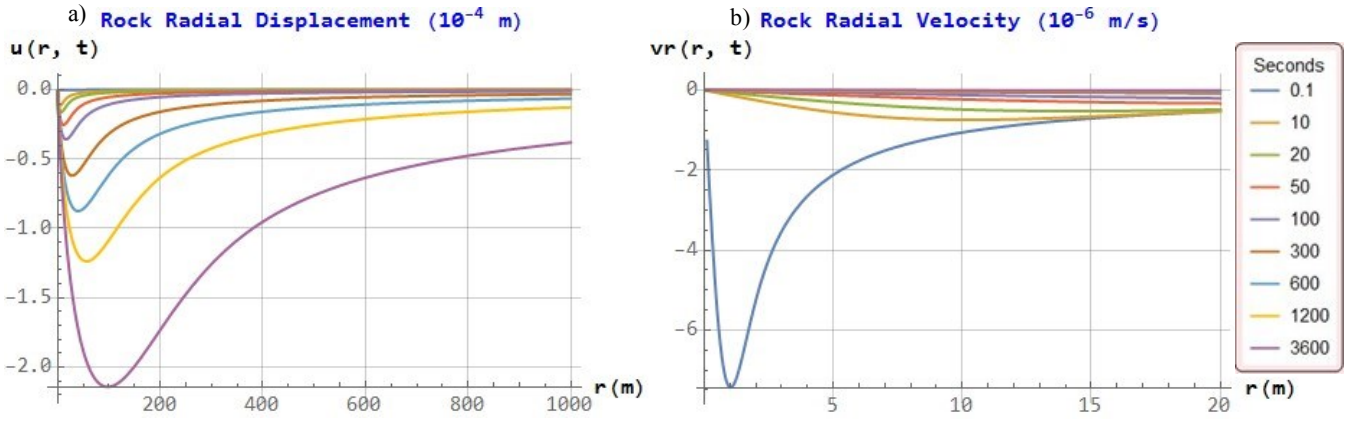

Figure 4: Radial displacement of the solid skeleton (left) and rock velocity (right) between 0.1 and 3600 seconds. Both vectors present negative values because the solid displacement occurs in the negative direction of the radial coordinate *r*.

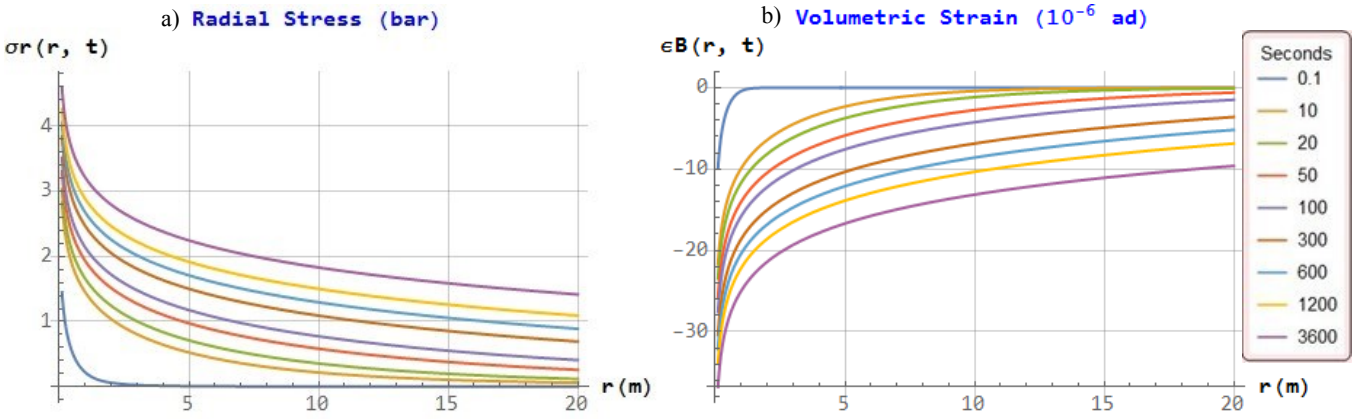

Figure 5: Radial stress (left) and volumetric strain (right) of the poroelastic rock between 0.1 and 3600 seconds. The values of σ_r correspond only to the extra stress (tension > 0) generated by the fluid extraction; the overburden pressure is about 300 bar. The strain $\varepsilon_B < 0$ because the solid displacements occur in the negative direction of the radial coordinates *r* and θ.

2.3 ThermoPoroelastic Results from the non-Isothermal Radial Model with Fluid Injection

If there are temperature differences (ΔT = 10°C) during fluid injection, it is necessary to add the effect of the thermal stress. Once both strains are known (Eq. 6), stresses and porosity are computed using equations (7) and (8) to include the effect of both pressure and temperature changes in the fluid/rock system. The following graphical results are obtained for an injection rate Q_v = + 0.05 m^3/s:

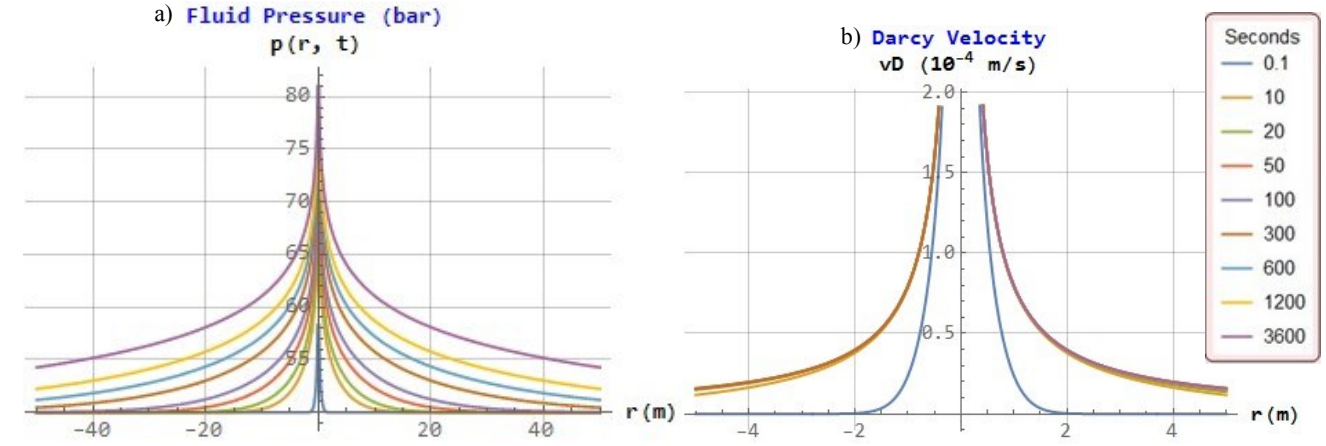

Figure 6: Fluid pressure (left) and radial Darcy velocity distribution (right) around the well, between 0.1 and 3600 seconds.

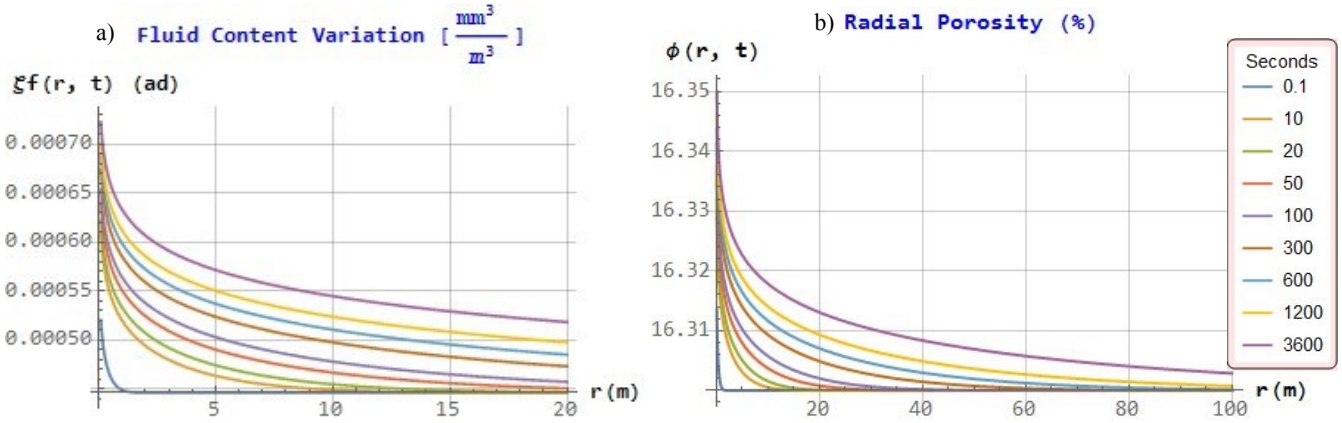

Figure 7: Fluid content variation (left) and rock porosity increment (right). Simulation times are between [0.1, 3600] seconds.

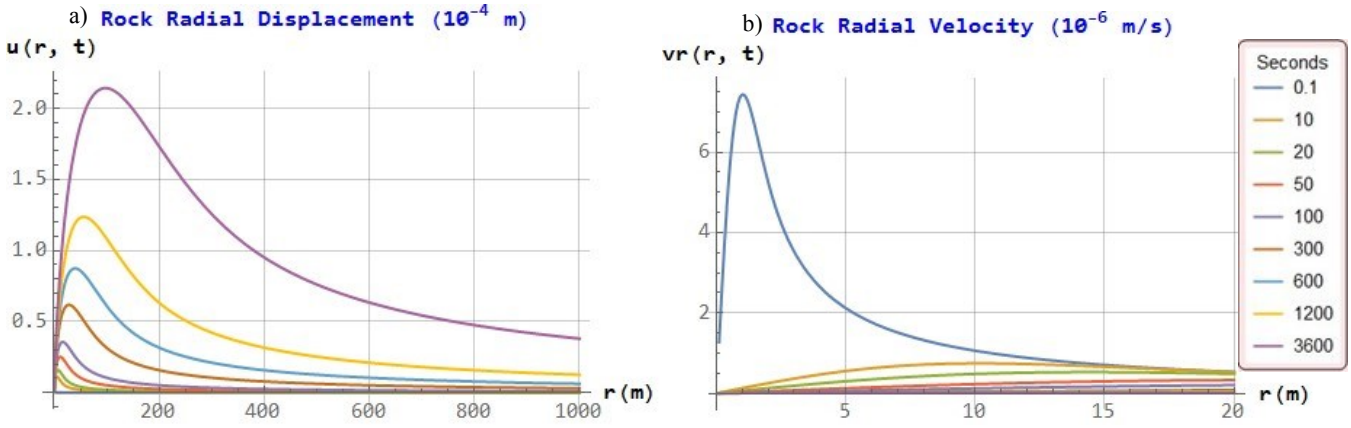

Figure 8: Radial displacement of the solid skeleton (left) and rock velocity (right) between 0.1 and 3600 seconds. Both vectors present positive values because the solid displacement occurs in the same direction of the radial coordinate $r > 0$ (Fig. 1).

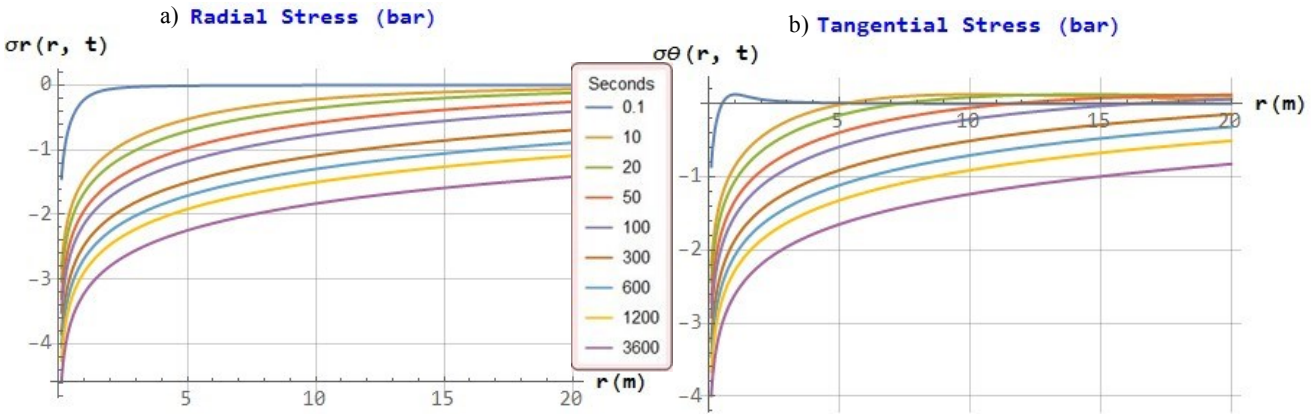

Figure 9: Radial (left) and tangential stress (right) in the poroelastic rock between 0.1 and 3600 seconds. The values of σ_r and σ_θ only represent the extra compression (< 0) generated by the fluid injection; the overburden pressure is about 300 bar. Both stresses are negative because they correspond to compressions acting on the porous rock in both directions.

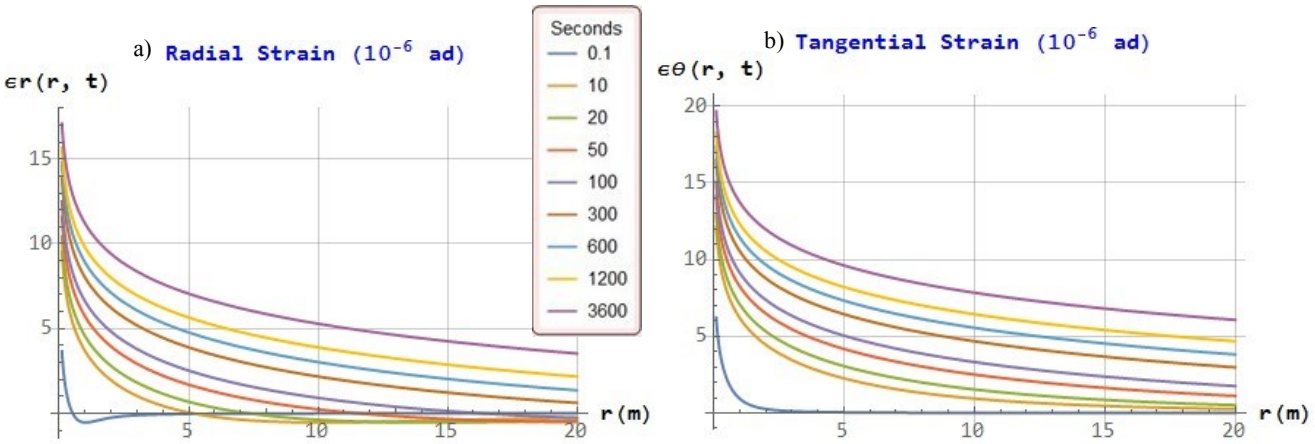

Figure 10: Radial (left) and tangential strain (right) of the poroelastic rock between 0.1 and 3600 seconds. Both strains are > 0 because the solid displacements occur in the positive direction of the radial coordinates *r* and *θ*.

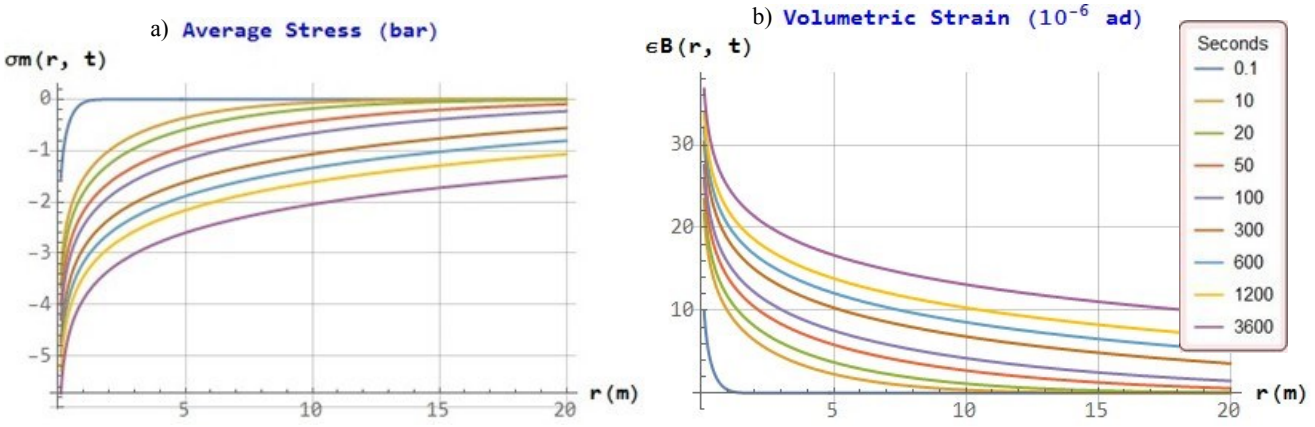

Figure 11: Average stress ($[\sigma_r + \sigma_\theta + \sigma_z]/3$, left) and volumetric strain (right) of the poroelastic rock between 0.1 and 3600 seconds. The values of σ_m correspond only to the extra compression in the rock generated by the fluid injection; the overburden pressure is about 300 bar. The strain $\varepsilon_B > 0$ because the solid displacements occur in the positive direction of the radial and tangential coordinates *r* and *θ*.

2.4 Brief Discussion of Graphical Results

The results obtained with the radial model, show and confirm several interesting experimental facts: first of all, fluid extraction or injection in a well (Figs. 2 and 6) produces poroelastic deformations (Figs. 4a, 5b, 8a and 10a,b). Even if they are of small magnitude, the strains and solid displacements are numerically detected at very early times, in the order of seconds (Figs. 4a, 5b, 8a, 10a,b and 11b). This occurs because the liquid flows through a porous rock whose solid skeleton can be deformed elastically instantaneously. Fluid extraction/injection in the reservoir causes the reduction/increment of the internal pore pressure (Figs. 2a and 6a) affecting both, the liquid content and the effective porosity (Figs. 3 and 7). Their magnitude is proportional to the volumetric flow rate (Eq. 4). A wave of non-negligible amplitude appears in the porous rock immediately after the fluid extraction/injection begins (Figs. 4b and 8b), but it is rapidly attenuated during the next simulation times. Therefore, the presence of the moving fluid in the porous rock modifies its mechanical response.

The internal tension produced by the liquid extraction (Fig. 5a), induces a decline of the fluid pressure and of the pore fluid content (Figs. 2a and 3a). The corresponding reduction of effective porosity (Fig. 3b) can be the principal source of liquid released from storage. When the poroelastic rock is subjected to internal compression because of injection (Figs. 6, 9 and 11a), the resulting matrix deformation leads to a volumetric increase of the pores containing the fluid (Figs. 7a,b and 11b). This increment of the pore volume must be bounded by physical poroelastic limits, defining a transitional zone before the rock enters the non-linear poroplastic region, where it can fail or be fractured. A practical condition for fracturing is given by the following empirical formula:

$$P_{frac}(t) \approx \sigma_\theta + p_I(t) \tag{9}$$

Where P_{frac} is the minimum pressure for the fracture to occur, σ_θ is the previously defined tangential stress (Eq. 8 and Fig. 9b) and p_I is the extra pressure of the injected fluid. This breaking pressure depends on several factors, specifically on the injection rate.

3. ANALYTICAL SOLUTIONS FOR TEMPERATURES IN THE RADIAL MODEL (LTNE)

In a pseudo-stationary state ($\partial/\partial t \sim 0$) for the temperatures of the solid and liquid phases, a Local Thermal Non-Equilibrium uncoupled radial model is obtained. Assuming that the temperature in the solid skeleton at $r = r_w$ is T_w, and at distance $r = r_L >> r_w$ is T_L, the analytic solution for the solid temperature $T_S(r)$ in radial coordinates for these boundary conditions is (see Appendix):

$$T_s(r) = \frac{\left(Q_S\left(r_L^2 - r_w^2\right) + 4\left(T_w - T_L\right)\delta_S\right)Ln(r) + \left(Q_S\left(r^2 - r_L^2\right) + 4T_L\,\delta_S\right)Ln(r_w) + \left(Q_S\left(r_w^2 - r^2\right) - 4T_w\,\delta_S\right)Ln(r_L)}{4\,\delta_S\,Ln\left(r_w / r_L\right)} \tag{10}$$

Where Q_s is the global solid heat transfer and δ_S is solid thermal diffusivity. The corresponding radial solution for the fluid temperature is (see Appendix):

$$T_f(r) = \frac{\left[\begin{array}{l} -E_i\left(\frac{r_L\,v_D}{\delta_f\,\varphi}\right)\left(\delta_f\,Q_f\,\varphi^2\,Ln\left(\frac{r}{r_w}\right) + v_D\left(Q_f\,\varphi\left(r - r_w\right) + T_w\,v_D\right)\right) + \\ + E_i\left(\frac{r_w\,v_D}{\delta_f\,\varphi}\right)\left(\delta_f\,Q_f\,\varphi^2\,Ln\left(\frac{r}{r_L}\right) + v_D\left(Q_f\,\varphi\left(r - r_L\right) + T_L\,v_D\right)\right) + \\ + E_i\left(\frac{r\,v_D}{\delta_f\,\varphi}\right)\left(\delta_f\,Q_f\,\varphi^2\,Ln\left(\frac{r_L}{r_w}\right) + v_D\left(Q_f\,\varphi\left(r_L - r_w\right) - \left(T_L - T_w\right)v_D\right)\right) \end{array}\right]}{v_D^2\left[E_i\left(\frac{r_w\,v_D}{\delta_f\,\varphi}\right) - E_i\left(\frac{r_L\,v_D}{\delta_f\,\varphi}\right)\right]} \tag{11}$$

Where Q_f is the fluid heat transfer and δ_f is fluid thermal diffusivity; $T_w = T_f(r_w)$ and $T_L = T_f(r_L)$ are the radial boundary conditions. The special function $E_i(x) = -E_1(-x)$ is another form of the classical exponential integral (Abramowitz & Stegun, 1972). Both equations (10) and (11) are coupled by the volumetric heat transfer coefficient q_{sf}:

$$Q_s = \frac{q_{sf} - q_s}{c_s\,\rho_s},\; Q_f = \frac{q_{sf}}{c_f\,\rho_f} \;\rightarrow\; \left[\frac{°C}{s}\right],\; \delta_S = \frac{k_s}{c_s\,\rho_s},\; \delta_f = \frac{k_f}{c_f\,\rho_f} \;\left[\frac{m^2}{s}\right] \tag{12}$$

Where c_s, c_f are solid and fluid specific heat, ρ_s, ρ_f and k_s, k_f are solid and fluid thermal conductivities respectively. All these terms are discussed in a previous paper (Suárez-Arriaga, 2016) and briefly redefined, in the Appendix.

The average temperature of the reservoir in pseudo-stationary state is:

$$T(r) = (1-\varphi)\, T_s(r) + \varphi\, T_f(r) \tag{13}$$

The corresponding graphics of both temperatures are:

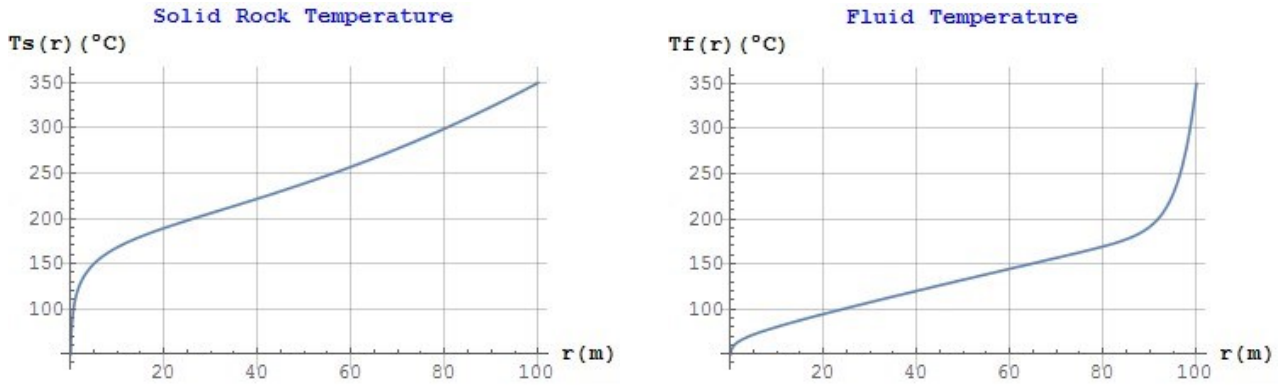

Figure 12: Solid (left) and Fluid (right) temperatures as functions of the radial coordinate *r*. The values of the heat transfers are Q_s = 0.1 °C/s and $Q_f = 0.5 \times 10^{-7}$ °C/s respectively; the Darcy velocity is $v_D = 0.7 \times 10^{-8}$ m/s. Other data used are in Table 1.

Equations (11) and (13) are valid for any values of the fluid velocity, Darcian or non-Darcian. The pseudo-stationary state is only valid for short injection times measured in minutes, or few hours. This approximation is not valid for larger residence times of the fluid.

4. CONCLUSIONS

Assuming the hypothesis of the classic Theis solution for pressure in a radial reservoir, an exact mathematical thermoporoelastic model was constructed. This model includes fluid flow, rock deformation and temperatures distribution. The total number of unknowns of the radial model are thirteen with the same number of equations. The results obtained show several interesting facts:

- The transport of a fluid in the reservoir modifies its mechanical response. Fluid extraction or injection in a well produces poroelastic deformations. Even if they are of small magnitude, the strains and solid displacements are detected at very early times, in the order of seconds, because the liquid flows through a porous rock whose solid skeleton can be deformed elastically in linear form.

- Fluid extraction or injection in the reservoir causes the reduction/increment of the pore pressure affecting both, the liquid content and the effective porosity in direct proportion to the volumetric flow rate.

- A wave of non-negligible amplitude appears in the vicinity of the well immediately after the fluid extraction/injection begins. This wave is rapidly attenuated.

- The internal tension produced by liquid extraction induces a decline of the fluid pressure and of the pore fluid content. There is a corresponding reduction of porosity that can be the principal source of liquid released from storage.

- The internal compression produced by fluid injection, causes a skeleton deformation that leads to a volumetric increase of the pores containing the fluid. This increment of porosity must be bounded by physical poroelastic limits, defining a transitional zone before the poroplastic region appears, where the rock can be fractured.

- This model can be useful to explore the start of a hydraulic fracturing process. Unpublished experimental data show that during a stimulation treatment performed in a low-permeability reservoir, which consisted in the injection of fluids at high pressure and flow rate into the formation interval of interest, a vertical fracture of 2.7 cm aperture was created after 300 seconds of continuous injection. The peak value of the injection pressure was 282 bar, which corresponded to the breaking pressure. After this peak, it was a pressure draw-down, which was stabilized at 160 bars during the next 10 hours of continuous injection.

- It is well known that hydraulic fracturing can create high-conductivity paths within a large area of the reservoir. The pressure increment caused by liquid injection induces the rock formation to fracture hydraulically. The breaking pressure required to induce fractures in a rock at a given depth can be estimated with this radial model if the maximum poroelastic radial displacement of the rock is known.

- This work is intended to explore the physical limits of a correct analytical solution of the thermoporoelastic problem in geothermal reservoirs. All the unknowns were successfully coupled in the isothermal poroelastic case. However, under local thermal non-equilibrium conditions the coupling is not possible using the exact model. The development of a numerical solution for the fully coupled non-isothermal case is a current research work in progress.

5. APPENDIX: CONSTRUCTION OF THE RADIAL MODEL

The basic equations governing the radial behavior of a linear thermoporoelastic rock are deduced from general principles and physical laws well established (Biot, 1941, 1955, 1972; Wang, 2000; Coussy, 2004; Bundschuh & Suarez-Arriaga, 2010; Vafai, 2015; Cheng, 2016). The main general principle is the equilibrium equation in poroelasticity:

$$\vec{\nabla} \cdot \boldsymbol{\sigma}_T (x_i, t) = 0 \tag{A0}$$

Where $\boldsymbol{\sigma}_T$ is the total stress tensor acting in the fluid-rock system. The strains in the solid skeleton are defined in terms of the components of the vector displacement of solid particles $\boldsymbol{u} = u_i(x_i)\, \boldsymbol{e}_i$:

$$\boldsymbol{\varepsilon}(x_i,t) = (\varepsilon_{ij}) = \frac{1}{2}\left(\frac{\partial u_i}{\partial x_j} + \frac{\partial u_j}{\partial x_i} \right) \tag{A1}$$

Where $\boldsymbol{\varepsilon}$ is the strain tensor and x_i represents any kind of coordinate, Cartesian, radial, etc. The equation relating stresses and strains is:

$$\sigma_{ij} = \lambda \varepsilon_B \delta_{ij} + 2G\varepsilon_{ij} - b(p_f - p_0)\delta_{ij} - K_B \gamma_B (T - T_0)\delta_{ij} \tag{A2}$$

Where ε_B $(= \varepsilon_{xx} + \varepsilon_{yy} + \varepsilon_{zz})$ is the volumetric strain, δ_{ij} is the unit tensor, λ and G are the Lamé and shear coefficients respectively for drained conditions, p_0, T_0 are the reservoir initial pore pressure and initial temperature, b is the Biot-Willis coefficient, K_B is the bulk modulus, and γ_B is the bulk thermal moduli; all coefficients are defined in the next section. Substituting equation (A2) into the equilibrium condition (A0) and using equation (A1) we obtain the first governing linear thermoporoelastic formula:

$$\left(K_B + \frac{G}{3} \right) \frac{\partial^2 u_i}{\partial x_i \partial x_j} + G \frac{\partial^2 u_i}{\partial x_j \partial x_j} - b \frac{\partial p_f}{\partial x_i} - K_B \gamma_B \frac{\partial T_s}{\partial x_i} = 0 \tag{A3}$$

Using the law of mass conservation and Darcy's law, the second governing equation for the fluid flow is obtained:

$$-\frac{k}{\mu_f} \frac{\partial^2 p_f}{\partial x_i \partial x_i} + \left(\frac{\varphi}{K_f} + \frac{b-\varphi}{K_s} \right) \frac{\partial p_f}{\partial t} + b \frac{\partial \varepsilon_B}{\partial t} = \left(\varphi \gamma_B + (b-\varphi)\gamma_\varphi \right) \frac{\partial T_f}{\partial t} \tag{A4}$$

Under the most general conditions of local thermal non-equilibrium or LTNE state ($T_s \neq T_f$), the heat transfer process between phases is modeled by the following two partial differential equations, one for the solid phase (s) and one for the fluid phase (f):

$$\frac{\partial}{\partial t}\left((1-\varphi) c_s \rho_s T_s \right) - (1-\varphi)\vec{\nabla} \cdot (\mathbf{k}_s \cdot \vec{\nabla} T_s) = (1-\varphi) q_s - (1-\varphi) q_{sf} \qquad \rightarrow \left[\frac{W}{m^3} \right] \tag{A5}$$

$$\frac{\partial}{\partial t}\left(\varphi c_f \rho_f T_f \right) - \varphi \vec{\nabla} \cdot (\mathbf{k}_f \cdot \vec{\nabla} T_f) + \vec{\nabla} \cdot (c_f \rho_f T_f \vec{v}_D) = \varphi q_{sf} \qquad \rightarrow \left[\frac{W}{m^3} \right] \tag{A6}$$

where t, φ, c, ρ, T, $\mathbf{k}$, $\boldsymbol{v}_D$, q_s and q_{sf} are time, porosity, heat capacity, density, temperature, conductivity tensor, Darcy velocity and volumetric heat generation of the solid (s) and fluid (f) phases respectively. The symbol q_{sf} is the amount of volumetric heat transferred from the solid matrix to the fluid and viceversa (Vafai, 2015; Suárez-Arriaga, 2016); this term is a function of the solid-fluid temperature difference (T_s - T_f); the volumetric heat q_{sf} depends also on a thermal coefficient and geometric variables. The microscopic fluid velocity in the pores $\boldsymbol{v}_f$, is related to the Darcy flux $\boldsymbol{v}_D$ by the Dupuit-Forchheimer relation $v_D = \varphi\, v_f$ (Bear, 1973).

The general equations (A2, A3, A4, A5, A6) include the energy transfer between the solid and the fluid phases at different temperatures; they correspond to a set of coupled equations governing general thermo-hydro-mechanical phenomena (THM) in porous rocks in LTNE. The main unknowns are, the vector displacement of the solid particles $\boldsymbol{u}$, the strain tensor $\boldsymbol{\varepsilon}$, the fluid pressure p_f and the fluid and rock temperatures T_f and T_s respectively. However, this linear formulation corresponds to a partial thermally uncoupled model, because both temperatures can be solved independently of the other unknowns if fluid velocity, porosity and initial and boundary conditions are known.

5.1 The Basic Radial Equations

If only radial coordinates are considered, all variables involved in the isothermal radial model are functions of radius and time [$f(r,t)$]. In non-isothermal conditions, the rock and liquid temperatures can be obtained as analytic functions of the radius only in a pseudo-stationary state. The vector displacement of the solid rock has only one component acting in the radial direction and, therefore its rotational is zero (Figure 13). The total number of unknowns in the radial model are thirteen, they are solved in the following algorithmic order:

$$\vec{u}_r = u_r(r,t)\vec{e}_r \;\rightarrow\; \nabla \times \vec{u}_r = 0 \;\rightarrow\; \boxed{p = p_f(r,t), \zeta_f, v_D, \vec{u}_r, \vec{v}_S, \varepsilon_r, \varepsilon_\theta, \varepsilon_B, \varphi, \overline{\sigma_r}, \sigma_\theta, T_f, T_S} \tag{A7}$$

where p_f, ζ_f, v_D, u_r, v_S, ε_r, ε_θ, ε_B, φ, σ_r, σ_θ, T_f, T_S, are fluid (pore) pressure, variation of the liquid content, Darcy velocity, solid displacement, solid deformation velocity, radial, tangential and bulk strains, porosity, radial and tangential stresses, fluid temperature and solid rock temperature, respectively.

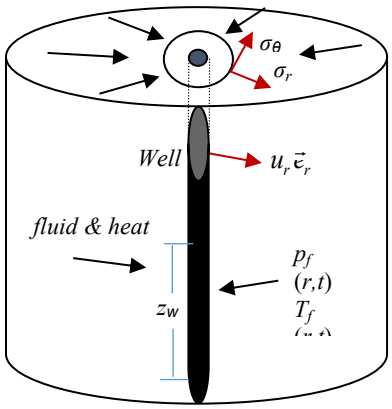

Figure 13: Radial geometry of an idealized reservoir showing its main elements and thermodynamic functions. Vector e_r indicates radial direction, r is the radius, t is current time and z_w is the length of the liner.

The liquid content variation ζ_f (increment or removal) can be measured experimentally or computed from poroelastic formulae. Under the condition of null rotational of the vector radial displacement, the variation of the fluid content ζ_f becomes proportional to the fluid pressure p_f (Wang, 2000; Cheng, 2016):

$$\vec{\nabla} \times \vec{u}_r(r,t) = \vec{0} \;\Rightarrow\; \boxed{\zeta_f(r,t) = S_r\, p_f(r,t)} \tag{A8}$$

Where S_r is the uniaxial specific fluid storage in the radial direction; it is calculated in terms of the radial compressibility $1/K_v$ and other poroelastic coefficients defined as follows:

$$\left\{ K_v = K_B + \frac{4}{3}G,\ \gamma_e = \frac{1+\nu_U}{1-\nu_U}\frac{B}{3} \right\} \;\Rightarrow\; \boxed{S_r = \frac{b}{K_v\,\gamma_e}} \tag{A9}$$

Where K_B, is the rock drained bulk modulus, G is the shear coefficient, γ_e is the poroelastic loading efficiency, ν_U is the undrained Poisson's coefficient, B is the Skempton coefficient, and b is the Biot-Willis (1957) modulus. If the fluid pressure satisfies the geometry and hypothesis of the infinite continuous line source (see Figure 13), then it can be computed with the modified Theis solution, from which Darcy velocity v_D is also deduced:

$$(\text{Theis model}) \;\rightarrow\; \eta_f = \frac{k_r}{\mu_f S_r},\ p_f(r,t) = p_0 + \frac{Q_v\,\mu_f}{4\pi z_w k_r} E_1\left[\frac{r^2}{4\eta_f t}\right] \;\Rightarrow\; v_D = -\frac{k_r}{\mu_f}\frac{\partial p_f}{\partial r} \tag{A10}$$

where η_f, p_0, Q_V, μ_f, z_w, k_r are hydraulic diffusivity, initial reservoir pore pressure, volumetric fluid flow rate, fluid viscosity, liner's length, and absolute radial permeability, respectively. The symbol E_1 is the classic exponential integral of degree 1

In radial coordinates the total stress tensor defined in equation (A2) becomes:

$$\boldsymbol{\sigma}_T = \begin{pmatrix} \sigma_r & 0 \\ 0 & \sigma_\theta \end{pmatrix} = \varepsilon_B \begin{pmatrix} \lambda & 0 \\ 0 & \lambda \end{pmatrix} + 2G \begin{pmatrix} \varepsilon_r & 0 \\ 0 & \varepsilon_\theta \end{pmatrix} - (p_f - p_0) \begin{pmatrix} b & 0 \\ 0 & b \end{pmatrix} - K_B (T - T_0) \begin{pmatrix} \gamma_B & 0 \\ 0 & \gamma_B \end{pmatrix} \tag{A11}$$

Where γ_B is the bulk thermal expansivity defined in next subsection. Porosity is defined as a bilinear function of the fluid pressure and reservoir temperature (Coussy, 2004; Bundschuh & Suarez-Arriaga, 2010), φ_0 is the initial porosity.

$$\varphi(r,t)=\varphi_0+b\,\varepsilon_B+\frac{p_f-p_0}{N_b}-\gamma_\varphi\left(T-T_0\right) \tag{A12}$$

Where N_b is the tangent Biot modulus, γ_φ is the thermal expansion coefficient of pores at constant p_f and defined in next subsection.

Physically, any applied radial stress σ_r generates a strain ε_r producing simultaneously a perpendicular tangential strain ε_θ, which corresponds to a tangential stress σ_θ (Figure 13). The strains of the radial displacement (A7) are deduced from the volumetric strain, which is equal to the divergence of the vector displacement $\boldsymbol{u}_r$:

$$\varepsilon_r+\varepsilon_\theta=\varepsilon_B(r,t)=\nabla\cdot\left(u_r\,\mathrm{r}\,\vec{e}_r\right)=\frac{\partial u_r}{\partial r}+\frac{u_r}{r}\;\Rightarrow\;\left\{\varepsilon_r=\frac{\partial u_r}{\partial r},\;\varepsilon_\theta=\frac{u_r}{r}\right\} \tag{A13}$$

5.2 The Theis Model in the Diffusion Equation for the Fluid Content Variation

This classical Theis mathematical model has the following initial, internal and external boundary conditions that are also satisfied by ζ_f:

$$\begin{aligned}&p_f(r,t)>0\;\rightarrow\;\frac{\partial p_f}{\partial t}=\eta_f\,\frac{\partial^2 p_f}{\partial r^2}+\frac{\eta_f}{r}\,\frac{\partial p_f}{\partial r},\;p_f(r,0)=p_0,\;\{\,\forall r\geq 0,\;t=0\,\}\\&\text{external \& internal boundaries: }\lim_{r\to\infty}p_f(r,t)=p_0,\;\lim_{r\to 0}\left(\frac{\partial p_f}{\partial r}\right)=\frac{Q_V\,\mu_f}{2\pi\,r_w z_w k_r}\end{aligned} \tag{A14}$$

The function ζ_f satisfies the same diffusion equation with appropriate initial and boundary conditions (Wang, 2000):

$$\frac{1}{\eta_f}\frac{\partial\zeta_f}{\partial t}=\nabla^2\zeta_f(r,t)\;\Rightarrow\;\left\{\zeta_f(r,0)=\zeta_0,\;\zeta_f(0,t)=\zeta_w,\;\zeta_f(\infty,t)=\zeta_0\right\} \tag{A15}$$

ζ_f also satisfies the following relationship in polar coordinates (Wang, 2000; Cheng, 2016):

$$\gamma_e\,\frac{\partial\zeta_f}{\partial r}=\frac{\partial}{\partial r}\left(\frac{1}{r}\,\frac{\partial(r\,u_r)}{\partial r}\right)\;\Rightarrow\;\left\{u_r(r,0)=0,\;u_r(0,t)\leq U_0,\;u_r(\infty,t)=0\right\} \tag{A16}$$

γ_e is the coupled poroelastic coefficient defined in equation (A9), η_f is the hydraulic diffusivity defined in equation (A10) assumed to be a function of the fluid temperature T_f only. The boundary and initial conditions in Eq. (A16) allows to integrate this equation exactly; the corresponding integration constants are eliminated, because u_r must be bounded for any value of (r, t):

$$\gamma_e\,\zeta_f(r,t)=c_1(t)+\left(\frac{1}{r}\,\frac{\partial(r\,u_r)}{\partial r}\right)\;\Rightarrow\;\gamma_e\int r\,\zeta_f\,\partial r=\frac{r^2}{2}\,\aleph_1(t)+r\,u_r(r,t)+\aleph_2(t)\;\Rightarrow\;u_r(r,t)=\frac{\gamma_e}{r}\int_0^r r\,\zeta_f(r,t)\,\partial r \tag{A17}$$

The irrotational condition for the solid displacement, implies that the liquid content variation ζ_f is proportional to the fluid pressure p_f, which can be computed with the Theis solution (Wang, 2000; Bundschuh & Suárez-Arriaga, 2010):

$$p_f(r,t)=p_0+\frac{Q_v\,\mu_f}{4\pi z_w k}\,E_1\left[\frac{r^2}{4\eta_f\,t}\right]\qquad(\text{Theis model})\;\Rightarrow\;\boxed{\zeta_f(r,t)=S_r p_0+\frac{S_r\,Q_v\,\mu_f}{4\pi z_w k}\,E_1\left[\frac{r^2}{4\eta_f\,t}\right]} \tag{A18}$$

The viscosity of liquid water grows slightly when pressure decreases, but its variability is larger when temperature changes. Therefore, Theis model in equation (A18) can be used for every isothermal curve with fixed porosity, and is approximately valid when both hydraulic diffusivity and porosity are updated for different fluid temperatures. It is interesting to mention here that S. Garg (1980) derived a simple diffusivity equation for the two-phase flow of water in geothermal systems. His model is valid for reservoirs of radial geometry with the same Theis' hypothesis, which assume a fully penetrating well in a very large homogeneous, isotropic reservoir of thickness z_w. The main hypothesis in Garg's model is that the reservoir is initially a two-phase system with uniform pressure and temperature everywhere. The resulting two-phase partial differential equation and its solution are completely analogous to Eqs. (A15) and (A18) for the liquid condition.

5.3 Computation of the Radial Displacement, Strains and Stresses

To obtain the solid radial displacement, the following procedure is used. The sudden injection of fluid at point (0, 0) is mathematically equivalent to the classic problem of an instantaneous line source with injection of heat at time t = 0, which satisfies the same diffusion

equation (A15) for ζ_f. The corresponding solution was obtained by Carslaw & Jaeger (1959, Chapter X, section 10.3) and is adapted here for ζ_f with a fluid line source of strength q_0:

$$\zeta_f^p(r,t) = \frac{q_0}{4\pi\eta_f t}\, e^{\frac{-r^2}{4\eta_f t}} \tag{A19}$$

Substituting this point source into equation (A16) the radial displacement corresponding to the sudden impulse produced in the solid skeleton by the instantaneous fluid line source is obtained as:

$$u_r^p(r,t) = \frac{q_0}{4\pi\eta_f t}\,\frac{\gamma_e}{r}\int_0^r r\, e^{\frac{-r^2}{4\eta_f t}}\, dr = \frac{q_0}{2\pi}\,\frac{\gamma_e}{r}\left(1 - e^{\frac{-r^2}{4\eta_f t}}\right) \tag{A20}$$

The radial displacement produced by an infinite continuous line source, corresponding to the Theis solution, is obtained by integrating equation (A20), replacing the value of the point source rate q_0 by the volumetric flow rate per unit length $Q_v\, dt / z_w$:

$$\boxed{u_r(r,t) = \frac{Q_v}{z_w}\int_0^t u_r^p\, dt = \frac{Q_v\,\gamma_e\, r}{8\pi\eta_f\, z_w}\left(\frac{4\eta_f t}{r^2}\left(1 - \mathrm{e}^{\frac{-r^2}{4\eta_f t}}\right) + \Gamma_0\left[\frac{r^2}{4\eta_f\, t}\right]\right)} \tag{A21}$$

Where Γ_0 is the incomplete Gamma function of order 0, a special function defined for a ≥ 0 (Abramowitz & Stegun, 1972) as follows:

$$\Gamma_a[w] = \int_w^\infty x^{a-1} e^{-x} dx \tag{A22}$$

The correctness of the solution given by equation (A21) can be verified calculating the partial derivative of $u_r(r, t)$ with respect to time t:

$$\frac{\partial}{\partial t}\Gamma_0\left[\frac{r^2}{4\eta_f\, t}\right] = \frac{1}{t}\,\mathrm{e}^{-\frac{r^2}{4t\eta_f}} \;\Rightarrow\; \frac{\partial}{\partial t}u_r(r,t) = \frac{Q_v\,\gamma_e}{8\pi\,\Delta z\, r}\left(4 - 4\,\mathrm{e}^{\frac{r^2}{4t\eta_f}}\right) = \frac{q_0}{2\pi}\,\frac{\gamma_e}{r}\left(1 - e^{\frac{-r^2}{4\eta_f t}}\right) = u_r^p(r,t) \tag{A23}$$

Once the radial displacement u_r is obtained from equation (A23), all the other unknowns can be computed directly with the relationships given by equations (A11, A12 and A13) in the order indicated by equation (A7). Darcy and solid velocities are easily computed:

$$\begin{aligned} \text{(Theis model)} \;\rightarrow\; v_D(r,t) &= -\frac{k_r}{\mu_f}\frac{\partial p_f}{\partial r} = \frac{Q_v}{2\pi z_w r}\,\mathrm{e}^{-\frac{r^2}{4\eta_f t}} \\ v_S(r,t) &= \frac{\partial u_r(r,t)}{\partial t} = \frac{Q_v\,\gamma_e}{2\pi z_w r}\left(1 - \mathrm{e}^{-\frac{r^2}{4\eta_f t}}\right) \end{aligned} \tag{A24}$$

5.3.1 Definitions of Experimental ThermoPoroelastic Coefficients

The coefficients introduced in previous equations are defined as follows. The variation of the fluid content ζ_f can be experimentally measured as (Biot, 1941; Wang, 2000):

$$\zeta_f(\rho_f, \varphi) = \frac{\rho_f\,\Delta\varphi + \varphi\,\Delta\rho_f}{\rho_0} \tag{A25}$$

where ρ_f is fluid density, φ is current porosity and ρ_0 is the initial fluid density. The thermal expansion coefficients, bulk modulus and compressibilities are defined as follows:

$$\gamma_\varphi = \frac{1}{\varphi}\left(\frac{\partial\varphi}{\partial T}\right)_{p_f},\; \gamma_B = -\frac{1}{\rho_s}\left(\frac{\partial\rho_s}{\partial T}\right)_{p_k},\; \frac{1}{K_f} = \frac{1}{\rho_f}\left(\frac{\partial\rho_f}{\partial p_f}\right)_T = C_f,\; K_B = \frac{1}{C_B} \tag{A26}$$

Where C_f, C_B, are fluid and bulk compressibilities respectively, and K_f is the bulk rock modulus. Biot moduli are defined next:

$$\frac{1}{M}=\left(\frac{\Delta\zeta_f}{\Delta p_f}\right)_{\varepsilon_B},\ b=\left(\frac{\partial p_k}{\partial p_f}\right)_{\varepsilon_B}=\left(\frac{\Delta V_\Phi}{\Delta V_B}\right)_{p_f},\ C=b\,M,\quad \frac{1}{N_b}=\frac{1}{M}-\frac{\varphi_0}{K_f} \tag{A27}$$

Detailed developments of all these moduli are described in (Bundschuh & Suárez-Arriaga, 2010 and Wang, 2000).

5.4 Analytical Solutions of Temperatures in the pseudo-Stationary LTNE Radial Model

Assuming a quasi-stationary state ($\partial/\partial t \sim 0$), equation (A5) in radial coordinates $T_S(r)$ becomes:

$$\boxed{\frac{1}{r}\frac{\partial}{\partial r}\left(r\frac{\partial T_S}{\partial r}\right)-\frac{Q_S}{\delta_S}=0},\quad \begin{cases}T_S\left(r=r_w\right)=T_w\\ T_S\left(r=L\right)=T_L\end{cases},\quad \delta_S=\frac{k_S}{c_s\,\rho_s} \tag{A28}$$

Where η_S is the thermal diffusivity of the solid rock. Integrating twice, the analytic solution for this PDE is simply:

$$T_s\left(r\right)=\frac{\left(Q_S\left(r_L^2-r_w^2\right)+4\left(T_w-T_L\right)\delta_S\right)Ln\left(r\right)+\left(Q_S\left(r^2-r_L^2\right)+4T_L\,\delta_S\right)Ln\left(r_w\right)+\left(Q_S\left(r_w^2-r^2\right)-4T_w\,\delta_S\right)Ln\left(r_L\right)}{4\,\delta_S\,Ln\left(r_w/r_L\right)} \tag{A29}$$

Where Q_S (°C/s) is the global solid heat transfer and δ_S is its thermal diffusivity in geothermal rocks. The conduction-convection heat partial differential equation equation for the liquid when the fluid flow is radial and quasi-stationary, with corresponding boundary conditions is:

$$\boxed{\frac{1}{r}\frac{\partial}{\partial r}\left(r\frac{\partial T_f}{\partial r}\right)-\frac{v_D}{\varphi\,\delta_f}\frac{\partial T_f}{\partial r}=-\frac{Q_f}{\delta_f}},\quad \begin{cases}T_f\left(r=r_w\right)=T_0\\ T_f\left(r=L\right)=T_L\end{cases},\quad \delta_f=\frac{k_f}{c_f\rho_f} \tag{A30}$$

Where δ_f is the thermal diffusivity of the fluid. Integrating twice and replacing the constant boundary conditions, the solution of this equation is:

$$T_f\left(r\right)=\frac{\left[\begin{array}{l}-E_i\left(\frac{r_L\,v_D}{\eta_f\,\phi}\right)\left(\eta_f\,Q_f\,\phi^2\,Ln\left(\frac{r}{r_w}\right)+v_D\left(Q_f\,\phi\left(r-r_w\right)+T_0\,v_D\right)\right)+\\ +E_i\left(\frac{r_w\,v_D}{\eta_f\,\phi}\right)\left(\eta_f\,Q_f\,\phi^2\,Ln\left(\frac{r}{r_L}\right)+v_D\left(Q_f\,\phi\left(r-r_L\right)+T_L\,v_D\right)\right)+\\ +E_i\left(\frac{r\,v_D}{\eta_f\,\phi}\right)\left(\eta_f\,Q_f\,\phi^2\,Ln\left(\frac{r_L}{r_w}\right)+v_D\left(Q_f\,\phi\left(r_L-r_w\right)-\left(T_L-T_0\right)v_D\right)\right)\end{array}\right]}{v_D^2\left[E_i\left(\frac{r_w\,v_D}{\eta_f\,\phi}\right)-E_i\left(\frac{r_L\,v_D}{\eta_f\,\phi}\right)\right]} \tag{A31}$$

Where E_i is another exponential integral defined as (Abramowitz & Stegun, 1972): $E_i[w]=\int_{-w}^{\infty}\frac{e^{-x}}{-x}\,dx$.

The average temperature in the reservoir at any time in the pseudo-stationary state is:

$$T\left(r\right)=\left(1-\varphi\right)T_s\left(r\right)+\varphi\,T_f\left(r\right) \tag{A32}$$

The previous equation is valid for typical values of the fluid velocity in pores and fractures and for short times measured in minutes or hours. The pseudo-stationary approximation is not valid for long residence times of the fluid.

5.4.1 Computing the radial displacement as function of pressure and temperature

The differential equation of the radial rock displacement $u_r(r, t)$ is defined as (Bundschuh & Suárez-Arriaga, 2010):

$$\left(K_B+\frac{4}{3}G\right)\left(\frac{\partial^2 u_r}{\partial r^2}+\frac{1}{r}\frac{\partial u_r}{\partial r}-\frac{u_r}{r^2}\right)-b\frac{\partial p_f(r,t)}{\partial r}-K_B\gamma_B\frac{\partial T_f(r)}{\partial r}=0 \tag{A33}$$

Solving by a special mathematical technique, this equation accepts a very large analytical solution in the functional form of:

$$u_r(r,t) = F\left(v_D,\ \delta_f,\ \varphi,\ r_L,\ r_w, u_w,\ T_L, T_w,\ Q_v,\ r,\ t,\ E_i\left[\frac{-r^2}{4\delta_f t}\right]\right) \tag{A34}$$

Where $u_w = u_r(r_w, 0)$; this solution is too large to include it here.

REFERENCES

Abramowitz, M. and Stegun, I.A. (eds): Handbook of mathematical functions with formulas, graphs, and mathematical tables. National Bureau of Standards, *Applied Mathematics Series* 55, issued June 1964, tenth printing, December 1972, with corrections, http://www.math.sfu.ca/~cbm /aands/ (accessed August 2009).

Biot, M.A.: General theory of three-dimensional consolidation. J. Appl. Physics 12 (1941), 155–164.

Biot, M.A.: Theory of elasticity and consolidation for a porous anisotropic solid. J. Appl. Physics 26 (1955), 182–185.

Biot, M.A.: Theory of finite deformations of porous solids. Indiana Univ. Math. J. 21:7 (1972), 597–620.

Biot, M.A. and Willis, D.G.: The elastic coefficients of the theory of consolidation. J. Appl. Mech. 24 (1957), 594–601.

Bundschuh, J. and Suarez-Arriaga, M.C.: Introduction to the Numerical Modeling of Groundwater and Geothermal Systems – Fundamentals of mass, energy and solute transport in poroelastic rocks. Vol. 2, Multiphysics Modeling Series, CRC Press – Taylor & Francis Group (2010).

Carslaw, H.S. and Jaeger, J.C.: *Conduction of heat in solids*. 2nd ed, Oxford Clarendon Press, Oxford, UK, (1959).

Cheng, A.H.D.: Poroelasticity, *Theory and Applications of Transport in Porous Media Series* Vol. 27, ed. Hassanizadeh, S.M. Founding series editor: Jacob Bear, (2016), Springer Int. Pub., http://www.springer.com/series/6612/ .

Coussy, O.: Poro mechanics. John Wiley & Sons, New York, NY, (2004).

Garg, S.K.: Pressure transient analysis for two-phase (water/steam) geothermal reservoirs. Society of Petroleum Engineers Journal, (1980), paper ***7479***, 206-214.

Suárez-Arriaga, M.C.: Local Thermal Non-Equilibrium Interfacial Interactions in Heterogeneous Reservoirs - Divergence of Numerical Methods to Simulate the Fluid and Heat Flow, *Proceedings,* 40th Workshop on Geothermal Reservoir Engineering, Stanford University, Stanford, CA (2016).

Vafai, K., (editor): Handbook of Porous Media, *CRC Press* – Taylor & Francis Group (2015).

Wang, H.F.: Theory of linear poroelasticity—with applications to geomechanics and hydrogeology. Princenton University Press, New Jersey, NJ, (2000).